IOP PUBLISHING JOURNAL OF PHYSICS G: NUCLEAR AND PARTICLE PHYSICS

J. Phys. G: Nucl. Part. Phys. **35** (2008) 065004 (11pp) doi:10.1088/0954-3899/35/6/065004

# Patterns of the exclusive double diffraction

**V A Petrov and R A Ryutin**

Institute for High Energy Physics, Theoretical Division, 142 281, Protvino, Moscow Region, Russian Federation

E-mail: Roman.Rioutine@cern.ch

Received 13 December 2007
Published 29 April 2008
Online at stacks.iop.org/JPhysG/35/065004

**Abstract**

We consider exclusive double diffractive events (EDDE) as a powerful tool to study the picture of the $pp$ interaction. Calculations of the cross-sections for the process $p + p \to p + M + p$ are presented in the convenient form for further experimental applications. We propose measurements of the diffractive $t$-distributions at the LHC. It is shown that important information on the interaction region could be extracted from the diffractive pattern.

(Some figures in this article are in colour only in the electronic version)

## 1. Introduction

With the first LHC run coming closer the hopes for confirmation of various theory predictions get heated. The huge amount of works is related to the search of fundamental particles of the Standard Model or its extensions (Higgs boson, superpartners, gravitons and so on) and to the investigations of the so-called hard QCD processes, which correspond to very short spacetime scales. 'Soft' diffractive processes take in this row its own, distinctive place.

LHC Collaborations aimed at working in low and high $p_T$ regimes related to typical undulatory (diffractive) and corpuscular (point-like) behaviours of the corresponding cross-sections may offer a very exciting possibility of observing an interplay of both regimes [1]. In theory the 'hard part' can be (hopefully) treated with perturbative methods whilst the 'soft' one is definitely nonperturbative.

Below we give several examples of such an interplay: exclusive particle production by diffractive scattered protons, i.e. the processes $p + p \to p + M + p$, where + means also a rapidity gap and $M$ represents a particle or a system of particles consisting of or strongly coupled to the two-gluon state [2].

These processes are related to the dominant amplitude of exclusive and semi-inclusive two-gluon production. The driving mechanism of the diffractive processes is the pomeron. Data on the total cross-sections unambiguously demand for the pomeron with larger-than-one intercept, thereof the need to take into account the 'soft' rescattering (i.e. 'unitarization').

  

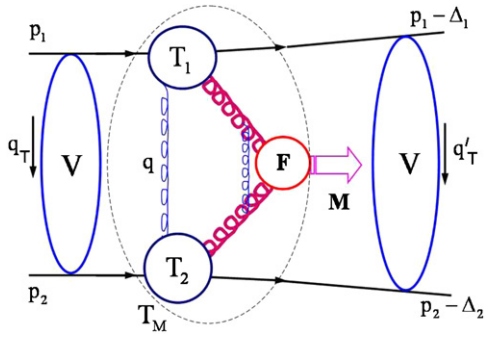


**Figure 1.** Model for EDDE.

Exclusive double diffractive events (EDDE) gives us unique experimental possibilities for particle searches and investigations of diffraction itself. This is due to several advantages of the process: (a) clear signature of the process; (b) possibility of using 'missing mass method' that improve the mass resolution; (c) background is strongly suppressed; (d) spin-parity analysis of the central system can be done; (e) interesting measurements concerning the interplay between 'soft' and 'hard' scales are possible. All these properties can be realized, for example, in common CMS/TOTEM detector measurements at LHC [3].

In the present paper, we discuss our new results on exclusive two gamma production and SM Higgs boson production. Also we propose measurements of the diffractive $t$-distributions at the LHC.

## 2. Exclusive double diffraction

The exclusive double diffractive process is related to the dominant amplitude of the exclusive two-gluon production. Driving mechanism of this process is the pomeron. There are several models and their modifications for EDDE [4–17]. Most of them are based on two different approaches for 'soft' (Regge-eikonal) and 'hard' (parton distributions in pomeron or proton, resummation of QCD diagrams, quasiclassical methods and so on) parts of the process. In contrast, we use the modification of the Regge-eikonal method for both parts.

To calculate an amplitude of the EDDE, we use an approach which was considered in detail in [2]. In the framework of this approach, the amplitude can be sketched as shown in figure 1. Proton–gluon amplitudes $T_{1,2}$ and proton–proton soft rescattering corrections $V$ are obtained in the Regge-eikonal approach [1] with three pomeron trajectories:

$$\begin{aligned}
\alpha_{IP_1}(t) - 1 &= (0.0578 \pm 0.002) + (0.5596 \pm 0.0078)t, \\
\alpha_{IP_2}(t) - 1 &= (0.1669 \pm 0.0012) + (0.2733 \pm 0.0056)t, \\
\alpha_{IP_3}(t) - 1 &= (0.2032 \pm 0.0041) + (0.0937 \pm 0.0029)t,
\end{aligned} \tag{1}$$

which are the result of 20 parameter fit of the total and differential cross-sections in the region 0.01 GeV$^2$ $< |t| <$ 14 GeV$^2$ and 8 GeV$< \sqrt{s} <$ 1800 GeV with $\chi^2$/d.o.f. $= 2.74$. Although $\chi^2$/d.o.f. is rather large, the model gives good predictions for the elastic scattering [1] (especially in the low-$t$ region), which was not included to the fit. It was also noted in [1] that this approach may be an artefact of the more general one with Regge cuts or nonlinear pomeron trajectory. Some attempts to find more universal solution were made in [18]. For $T_{1,2}$ the model is extended to off-shell particles [19]. As was shown in [20] the main contribution

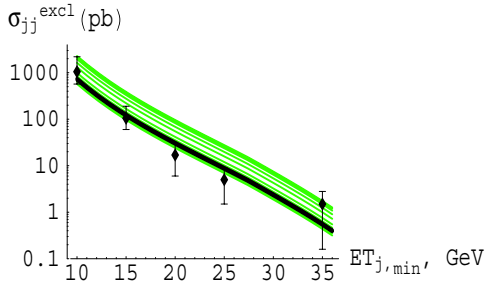


**Figure 2.** The latest data from CDF and predictions for EDDE.

**Table 1.** Phenomenological parameters of the 'hard' pomeron trajectory obtained from the fitting of the HERA and Tevatron data (see [2, 20]), and data on $pp$ ($p\bar{p}$) scattering [1]. The value of the $c_{gp}$ is obtained by the fit of the latest data from CDF [23], which is depicted in figure 2 with the range of possible curves. The previous value $c_{gp} = 3.5 \pm 0.4$ [20] is different, but within errors of the new one.

| $\alpha_{I\!P_3}(0)$ | $\alpha'_{I\!P_3}(0)$ (GeV$^{-2}$) | $r^2_{pp}$ (GeV$^{-2}$) | $r^2_{gp}$ (GeV$^{-2}$) | $c_{gp}$ |
|---|---|---|---|---|
| $1.2032 \pm 0.0041$ | $0.0937 \pm 0.0029$ | $2.4771 \pm 0.0964$ | $2.54 \pm 0.41$ | $3.2 \pm 0.5$ |

to the proton–gluon amplitude is given by the third (we call it 'hard' in this paper, and this is not the usual DL one [21]) pomeron.

After the tensor contraction of the amplitudes $T_{1,2}$ with the gluon–gluon fusion vertex, the full 'bare' amplitude $T_M$ depicted in figure 1 looks like

$$T_M = \frac{2}{\pi} c_{gp}^2 \, \mathrm{e}^{b(t_1+t_2)} \left(-\frac{s}{M^2}\right)^{\alpha_{I\!P_3}(0)} F_{gg\to M} I_s. \tag{2}$$

Here

$$b = \alpha'_{I\!P_3}(0) \ln\left(\frac{\sqrt{s}}{M}\right) + b_0, \tag{3}$$

$$b_0 = \frac{1}{4}\left(\frac{r^2_{pp}}{2} + r^2_{gp}\right), \tag{4}$$

with the parameters of the 'hard' pomeron trajectory, that appears to be the most relevant in our case, presented in table 1. By default we use the parameters of table 1 for our calculations. The last factor on the rhs of (2) is

$$I_s = \int_0^{\mu^2} \frac{\mathrm{d}l^2}{l^4} F_s(l^2, \mu^2) \left(\frac{l^2}{s_0 + l^2/2}\right)^{2\alpha_{I\!P_3}(0)}, \tag{5}$$

where $l^2 = -q^2 \simeq \mathbf{q}^2$, $\mu = M/2$ and $s_0 = 1$ GeV$^2$ is a fixed scale parameter of the model which is also used in the global fitting of the data on $pp$ ($p\bar{p}$) scattering for on-shell amplitudes [1]. If we take into account the emission of virtual 'soft' gluons, while prohibiting the real ones, that could fill rapidity gaps, it results in a Sudakov-like suppression [22]:

$$F_s(l^2, \mu^2) = \exp\left[-\int_{l^2}^{\mu^2} \frac{\mathrm{d}p_T^2}{p_T^2} \frac{\alpha_s(p_T{}^2)}{2\pi} \int_\Delta^{1-\Delta} z P_{gg}(z)\,\mathrm{d}z + \int_0^1 \sum_q P_{qg}(z)\,\mathrm{d}z\right], \tag{6}$$

$$P_{gg}(z) = 6\frac{(1-z(1-z))^2}{z(1-z)}, \tag{7}$$

$$\Delta = \frac{p_T}{p_T+\mu}. \tag{8}$$

The amplitude $F_{gg\to M}$ is the usual gluon–gluon fusion amplitude calculated perturbatively in the SM or in its extensions.

The data on total cross-sections unambiguously demand the pomeron with larger-than-one intercept, thereof the need in unitarization. The amplitude with unitary corrections, $T_M^{\text{unit}}$, is depicted in figure 1. It is given by the following analytical expressions:

$$T_M^{\text{unitar}}(p_1, p_2, \Delta_1, \Delta_2) = \frac{1}{16ss'}\int \frac{\mathrm{d}^2\mathbf{q}_T}{(2\pi)^2}\frac{\mathrm{d}^2\mathbf{q}'_T}{(2\pi)^2}V(s,\mathbf{q}_T) \times T_M(p_1-q_T, p_2+q_T, \Delta_{1T}, \Delta_{2T})V(s',\mathbf{q}'_T), \tag{9}$$

$$V(s,\mathbf{q}_T) = 4s(2\pi)^2\delta^2(\mathbf{q}_T) + 4s\int \mathrm{d}^2\mathbf{b}\,\mathrm{e}^{\mathrm{i}\mathbf{q}_T\mathbf{b}}[\mathrm{e}^{\mathrm{i}\delta_{pp\to pp}}-1], \tag{10}$$

where $\Delta_{1T} = \Delta_1 - q_T - q'_T$, $\Delta_{2T} = \Delta_2 + q_T + q'_T$, and the eikonal function $\delta_{pp\to pp}$ can be found in [1]. The left and right parts of the diagram in figure 1 denoted by $V$ represent 'soft' re-scattering effects in the initial and final states, i.e. multi-pomeron exchanges. As was shown in [24], these 'outer' unitary corrections strongly reduce the value of the corresponding cross-section and change an azimuthal angle dependence.

In equation (2) we only present the Born terms from amplitudes $T_{1,2}$. It is sufficient for $|t_{1,2}| < 1$ GeV due to the fast decrease of the differential cross-section in $t_{1,2}$, and the contribution of these corrections to the total cross-section are less than several per cents. But when we consider the diffractive pattern in the region of $1 < |t_{1,2}| < 5$ GeV, we have to take into account rescattering corrections inside the amplitudes $T_{1,2}$. In this case $I_s$ in equation (2) changes to the following expression:

$$I_s^{\text{corr}} = \int_0^{\mu^2}\frac{\mathrm{d}l^2}{l^4}F_s(l^2)\left(\frac{l^2}{s_0+l^2/2}\right)^{\alpha_{IP_3}(t_1)+\alpha_{IP_3}(t_2)}(1+h(v,t_1))(1+h(v,t_2)), \tag{11}$$

$$h(v,t) = \sum_{n=2}^{\infty}\frac{(-1)^{n-1}}{n!\times n}\left(\frac{c_{gp}}{8\pi b_1(v)}\exp\left[-\frac{\mathrm{i}\pi(\alpha_{IP_3}(0)-1)}{2}\right]v^{\alpha_{IP_3}(0)-1}\right)^{n-1} \times \exp\left[\frac{b_1(n-1)}{n}|t|\right], \tag{12}$$

$$v = \frac{\sqrt{s}}{M}\frac{l^2}{s_0+l^2/2}, \tag{13}$$

and $b$ to

$$b_1 = \alpha'_{IP_3}(0)\ln v + b_0. \tag{14}$$

To calculate the differential and total cross-sections for exclusive processes we can use the formula

$$M^2\frac{\mathrm{d}\sigma^{\text{EDDE}}}{\mathrm{d}M^2\,\mathrm{d}y\,\mathrm{d}\Phi_{gg\to M}}\bigg|_{y=0} = \hat{L}^{\text{EDDE}}\frac{\mathrm{d}\hat{\sigma}^{J_z=0}}{\mathrm{d}\Phi_{gg\to M}}, \tag{15}$$

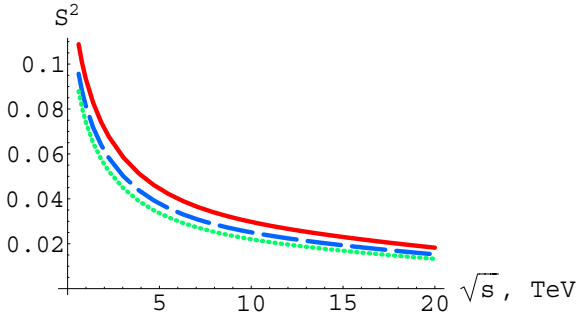


**Figure 3.** 'Soft' survival probability $S^2$ as a function of $\sqrt{s}$ for masses of the central system 10 GeV (solid curve), 50 GeV (dashed) and 200 GeV (dotted).

$$\hat{L}^{\mathrm{EDDE}} = \frac{c_{gp}^4}{2^5\pi^6}\left(\frac{s}{M^2}\right)^{2(\alpha_{IP_3}(0)-1)}\frac{1}{4b^2}I_s S^2, \tag{16}$$

$$S^2 = \frac{\int \mathrm{d}^2\vec{\Delta}_1\,\mathrm{d}^2\vec{\Delta}_2|T_M^{\mathrm{unitar}}|^2}{\int \mathrm{d}^2\vec{\Delta}_1\,\mathrm{d}^2\vec{\Delta}_2|T_M|^2}, \tag{17}$$

where $\mathrm{d}\hat{\sigma}^{J_z=0}/\mathrm{d}\Phi_{gg\to M}$ is the 'hard' exclusive singlet gluon–gluon fusion cross-section and $S^2$ is the so-called soft survival probability. In this work, the quantity $\hat{L}$ is called $g^{IP}g^{IP}$ luminosity.

The factor $S^2$ is depicted in figure 3 for the systems $M$ with quantum numbers $0^{++}$ (SM Higgs boson, radion, jet–jet). For other cases it is of the same order and can be calculated using the Monte Carlo event generator EDDE [25].

## 3. Results

First of all we would like to discuss some features of the process $pp \to p+\gamma\gamma+p$, since this process is the standard one to obtain the model parameters. Cross-sections for this process are presented in figure 4. It is important to note that the cut $E_{T\gamma} > E_{\mathrm{cut}} = M_{\mathrm{cut}}/2$ is used in the major part of experimental works, that is why we have to use the same one in our calculations. But in some theoretical works [26] $E_T > E_{\mathrm{cut}}$ means another cut $M_{\gamma\gamma} > 2E_{\mathrm{cut}}$, which leads to the result, similar to that presented in figure 4(b). In this figure, cross-section for $|\eta_\gamma| < 2$ is about two times higher than for $|\eta_\gamma| < 1$. Such a difference is only possible in the kinematics, when $M_{\gamma\gamma} > 2E_{\mathrm{cut}}$. It follows from rather simple calculations. The total cross-section for the process $gg \to \gamma\gamma$ can be represented as [27]

$$\hat{\sigma}^{J_z=0}_{gg\to\gamma\gamma}(M_{\gamma\gamma}, \eta_{\max}) = C_{\gamma\gamma}F(\eta_{\max})\frac{\alpha_s(M_{\gamma\gamma}/2)^2}{M^2_{\gamma\gamma}}, \tag{18}$$

where $\eta_{\max}$ is the pseudorapidity cut in the central mass frame of the diphoton system, $C_{\gamma\gamma}$ is the constant,

$$F(\eta_{\max}) = \int_{-\eta_{\max}}^{\eta_{\max}}\frac{\mathrm{d}\eta}{\mathrm{ch}^2\eta}\left[1+\left(1-2\eta\,\mathrm{th}\,\eta+\frac{1}{4}(\pi^2+4\eta^2)(1+\mathrm{th}^2\eta)\right)^2\right] \tag{19}$$

is depicted in figure 5(a). And for the process $pp \to p+\gamma\gamma+p$ from (15) we have

$$\sigma_{pp\to p+\gamma\gamma+p}(E_{\mathrm{cut}}, \eta_{\max}) \simeq \int_{2E_{\mathrm{cut}}}^{\sqrt{\xi_{1\max}\xi_{2\max}s}}\frac{\mathrm{d}M^2}{M^2}\hat{L}^{\mathrm{EDDE}}(M)\hat{\sigma}^{J_z=0}_{gg\to\gamma\gamma}(M, \eta_{\max})\Delta y. \tag{20}$$

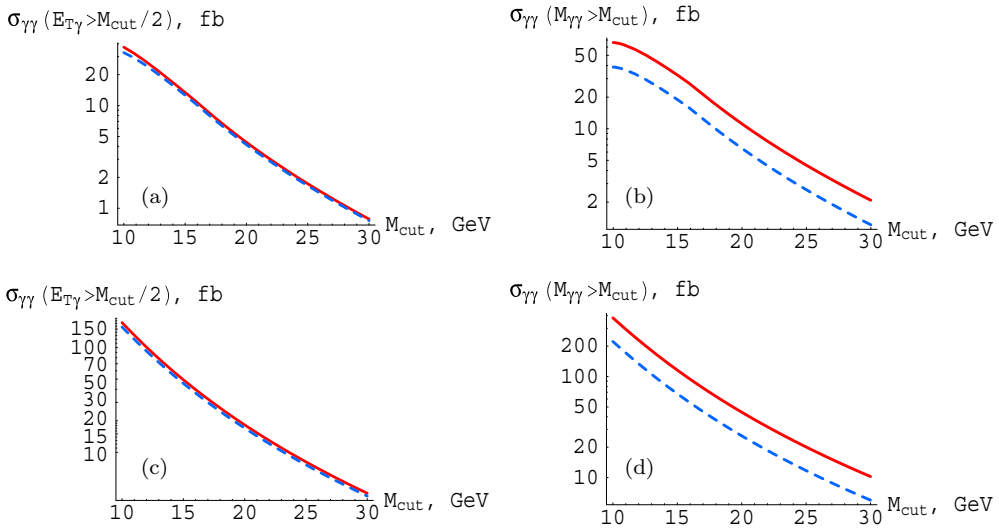


**Figure 4.** Cross-sections for the process $pp \to p + \gamma\gamma + p$ for different kinematical cuts. The solid and dashed curves correspond to the pseudorapidity cuts $|\eta_\gamma| < 2$ and $|\eta_\gamma| < 1$: (a) $\sqrt{s} = 1.8$ TeV, CDF cuts for $\xi_{1,2}$ [23], and cut on the $E_{T\gamma}$; (b) $\sqrt{s} = 1.8$ TeV, CDF cuts for $\xi_{1,2}$ [23], and cut on the $M_{\gamma\gamma}$; (c) $\sqrt{s} = 14$ TeV, symmetric cuts $0.0003 < \xi_{1,2} < 0.1$, and cut on the $E_{T\gamma}$; (d) $\sqrt{s} = 14$ TeV, symmetric cuts $0.0003 < \xi_{1,2} < 0.1$, and cut on the $M_{\gamma\gamma}$.

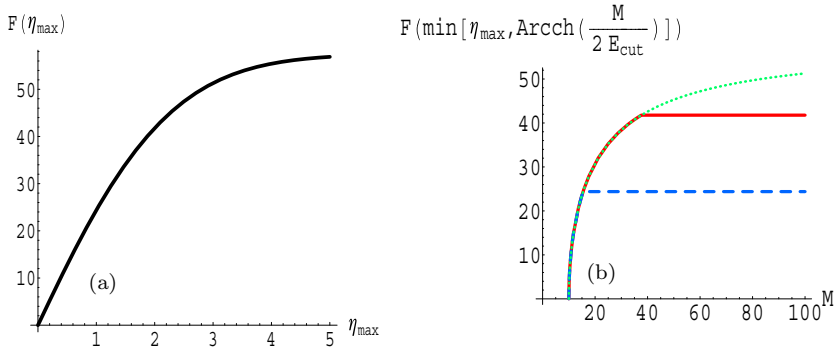


**Figure 5.** (a) Function $F(\eta_{\max})$; (b) $\eta_{\max} = 2$ (solid curve), $\eta_{\max} = 1$ (dashed), $F\left(\mathrm{Arcch}\frac{M}{2E_{\rm cut}}\right)$ (dotted), $E_{\rm cut} = 5$ GeV.

We are interested in the ratio of total cross-sections for different $\eta_{\max}$. Let us consider first the kinematics with cuts

$$M_{\gamma\gamma} > 2E_{\rm cut}, \qquad |\eta_\gamma| < \eta_{\max}. \tag{21}$$

In this case,

$$\frac{\sigma_{pp\to p+\gamma\gamma+p}(M > 2E_{\rm cut}, |\eta| < 2)}{\sigma_{pp\to p+\gamma\gamma+p}(M > 2E_{\rm cut}, |\eta| < 1)} \simeq \frac{F(2)}{F(1)} \simeq 1.7. \tag{22}$$

**Table 2.** Rates for the exclusive Higgs production and different backgrounds at the integrated luminosity 100 fb$^{-1}$ and $\Delta M_{\text{missing}} = 4$ GeV. The probability to misidentify gluon jets with b-jets is taken to be 1%.

| Process | $N$ events $c_{gp} = 3.2$ | $N$ events $c_{gp} = 2.7$ | $N$ events $c_{gp} = 3.7$ |
|---|---|---|---|
| $\sigma^{\text{EDDE}}(H \to b\bar{b})$ | 15 | 7 | 27 |
| $\sigma^{SI}(H \to b\bar{b})$ | 1 | 0 | 2 |
| $\sigma^{\text{EDDE}}(b\bar{b})$ | 7 | 3 | 12 |
| $\sigma^{\text{EDDE}}(b\bar{b}g)$ | 1 | 0 | 1 |
| $\sigma^{\text{EDDE}}(gg) \times 10^{-4}$ | 8 | 4 | 14 |
| $\sigma^{\text{EDDE}}(ggg) \times 10^{-4}$ | 1 | 0 | 2 |
| Signal/Background | 0.83 | 1 | 0.87 |

Since in the central mass frame of the diphoton system we have $M_{\gamma\gamma} = 2E_{T\gamma}\,\text{ch}\,\eta_\gamma$, in the kinematics with

$$E_{T\gamma} = \frac{M_{\gamma\gamma}}{2\text{ch}\eta_\gamma} > E_{\text{cut}}, \qquad |\eta_\gamma| < \eta_{\max} \tag{23}$$

we have additional cut

$$|\eta_\gamma| < \text{Arcch}\frac{M_{\gamma\gamma}}{2E_{\text{cut}}}, \tag{24}$$

and we should use $F\big(\min\big[\eta_{\max}, \text{Arcch}\frac{M_{\gamma\gamma}}{2E_{\text{cut}}}\big]\big)$ instead of $F(\eta_{\max})$ in (18). This new function is shown in figure 5(b). The main contribution to the integral comes from small masses due to fast decrease in $M$, but in this region we have the same cut $|\eta| < \text{Arcch}\frac{M}{2E_{\text{cut}}}$ for different $\eta_{\max}$. And it is easy to get the following result:

$$\frac{\sigma_{pp\to p+\gamma\gamma+p}(E_T > E_{\text{cut}}, |\eta| < 2)}{\sigma_{pp\to p+\gamma\gamma+p}(E_T > E_{\text{cut}}, |\eta| < 1)} \simeq 1.1 \qquad \text{for} \quad E_{\text{cut}} = 5\ \text{GeV}. \tag{25}$$

Even if we take $\alpha_s = \text{const}$ and $\hat{L}^{\text{EDDE}} = \text{const}$, we will get the ratio 1.3, and not $\sim$2 as in [26]. This simple example shows that we should be careful with the kinematics during our calculations, since this could lead to different predictions. Now we can compare our result with the latest data on the exclusive $\gamma\gamma$ production from CDF [28]:

$$\sigma_{pp\to p+\gamma\gamma+p}(E_{T\gamma} > 5\,\text{GeV}, |\eta_\gamma| < 2) = 0.14^{+0.14}_{-0.04}(\text{stat.}) \pm 0.03(\text{syst.})\,\text{pb}. \tag{26}$$

This prediction is higher than our calculations based on the di-jet production [23]. If we believe in this result, the model parameter $c_{gp}$ is at least 20% higher than our estimations. The possible reason is that in $\gamma\gamma$ production we use the region of small masses for the normalization of our parameter (and higher masses for the di-jet production), but the uncertainty in the scale dependence of the cross-section is rather large (factor $\sim$2). This result from CDF may serve as a good signal for the future exclusive Higgs boson production, since it makes the cross-section higher by about two times.

Now we can estimate the backgrounds for the exclusive Higgs production at LHC [2]. Rates for these processes at the integrated luminosity 100 fb$^{-1}$ are summarized in table 2 (to estimate uncertainties of the prediction based on [23], we obtain results for $c_{gp} = 3.2, 2.7, 3.7$). From this table, we can obtain the signal-to-background ratio $\sim$1. More exact estimations will be made in the nearest future after full Monte Carlo simulations.

## 4. Diffractive patterns

In the general agenda of the LHC experiment diffraction often appears as an 'auxiliary tool' for other processes such as Higgs boson and exotics searches, background suppression and so on. Nevertheless, diffractive measurements have their own classical tasks directly related to the angular (or $t$) distributions.

The diffractive pattern is usually characterized by the peak at small values of $t$, and complicated structure with dips or breaks and bumps for larger $t$ [1]. This picture reflects the undulatory properties of quantum processes in contrast to more habitual particle-like behaviour and allows us to get an information about the size and shape of the strong interaction region at large distances (i.e. directly related to confinement of the QCD colour fields).

- From the diffractive pattern we extract model-independent parameters of the interaction region such as the $t$-slope which is $R^2/2$, with $R$ being the transverse radius of the interaction region.
- We can also estimate the longitudinal size of the interaction region [29]:

$$\Delta x_L > \frac{\sqrt{s}}{2\sqrt{\langle t^2\rangle - \langle t\rangle^2}}. \tag{27}$$

  The longitudinal interaction range is somehow 'hidden' in the amplitude but it is this range that is responsible for the 'absorption strength'. A rough analogue is the known expression for the radiation absorption in media which critically depends on the thickness of the absorber.
- The very presence of dips is the signal of the quantum interference of hadronic waves.
- The depth of dips is determined by the real part of the scattering amplitude.

According to the data from $Sp\bar{p}S$ and Tevatron the transverse radius of the interaction region is of the order of 1.2 fm $\simeq 1.5\langle r_{\rm em}\rangle$. The longitudinal size can be estimated from the second inequality (27). For example, for the $e^{Bt}$ distribution with the slope $B \simeq 4$,

$$\Delta x_L > \frac{B\sqrt{s}}{2} \simeq 28\,000\,\text{GeV}^{-1} \simeq 5600\,\text{fm}. \tag{28}$$

The diffractive pattern moves due to changes in kinematical parameters such as the energy of the interaction or an additional hard scale. This motion reflects the dynamics of the process. The increase of the $t$-slope with energy reflects the growth of the interaction radius. At fixed collision energy the diffractive pattern is fixed as well.

However if we have in our disposal an additional hard scale we can operate the diffractive pattern adjusting this hard scale at our will and making, e.g., the interaction region larger or smaller.

Hard scale is related to small distances and, from the simple optical point of view, the pattern should move towards large values of $-t$ with the increase of the hard scale. HERA provides an excellent opportunity to observe the influence of a hard scale ($Q^2$) on the diffractive pattern: the slope decreases with $Q^2$ in exclusive vector meson or photon production or for mesons containing heavy quarks ($J/\Psi$) as contrasted to those composed of the light quarks (see figure 6) [30].

The decrease of the slope with $Q^2$ in electroproduction was predicted qualitatively in [31]: J D Bjorken argued that the decrease of the slope would be bounded from below by the size of nucleon [32]. The latter feature seems to be violated in the HERA data [33], but could also be interpreted by the fact that the gluonic core has the size $0.65 \pm 0.02$ fm and sits well inside the electromagnetic radius of the proton. We have to mention that the presence of a high-mass particle in the final state does not always lead to the phenomena described above.

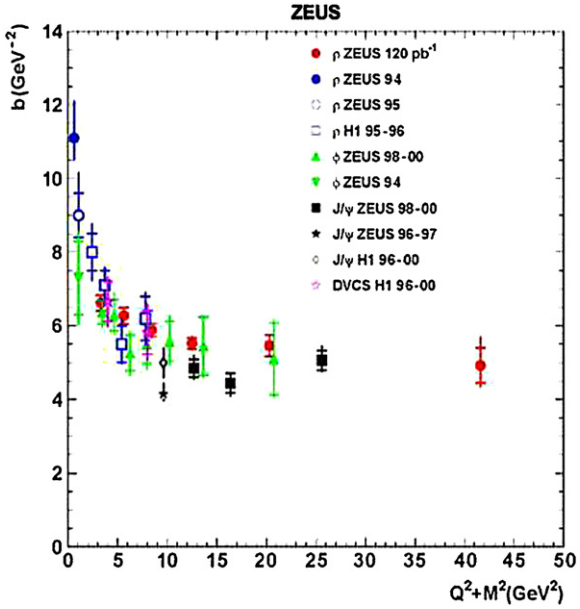


**Figure 6.** The slope $b$ as a function of $Q^2 + M_V^2$.

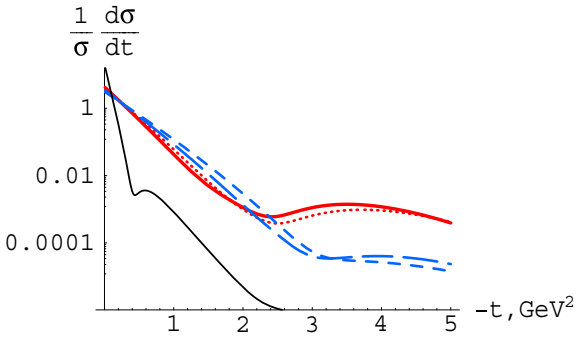


**Figure 7.** Normalized cross-section for exclusive di-jet production as a function of $t$ for $M_X = 30$ GeV (the solid and long-dashed curves correspond to the LHC and TEVATRON energies, respectively) and $M_X = 200$ GeV (the dotted and short-dashed curves correspond to the LHC and TEVATRON energies, respectively). The left curve corresponds to the elastic scattering at the LHC.

For example, hadronic resonances with large masses have large size due to intrinsic motion of constituents, and cannot be considered as a hard probe. In this case, we have inverse dynamics of the pattern [34]. This certainly is not the case for the processes considered below as they are related exclusively to short-distance probes, i.e. 'high mass' means always 'high $E_T$'.

The diffractive pattern for the process $p + p \to p + jj + p$ as predicted on the basis of [2] is displayed in figure 7 where $\frac{1}{\sigma}\frac{d\sigma}{dt}$ means the exclusive differential cross-section with all final variables integrated except one of the proton transverse momenta $(-t)$ and the value of the central mass ($M \simeq 2E_T$). With two exclusive high-$E_T$ jets the expected dips will reflect

**Table 3.** Rates for exclusive and semi-inclusive ($|\eta_{\rm soft}| < 5$) double diffractive di-jet production for luminosity $10^{33}$ cm$^{-2}$ s$^{-1}$ for different intervals of the invariant mass of the central system, $M_X$. Effective $t$-slopes are calculated in the model developed in this paper.

| $M_1 < M_X < M_2$ (GeV) | $t$-slope (GeV$^{-2}$) | $N_{\rm ex}$ | $N_{\rm semi\text{-}incl.}$ |
|---|---|---|---|
| $29 < M_X < 31$ | $4.64 \pm 0.32$ | $2 \times 10^4$ per day | $6 \times 10^4$ per day |
| $98 < M_X < 102$ | $4.31 \pm 0.31$ | $9 \times 10^3$ per month | $4.5 \times 10^4$ per month |
| $196 < M_X < 204$ | $4.12 \pm 0.31$ | $5.5 \times 10^3$ per year | $4 \times 10^4$ per year |

the elastic scattering of the protons off the hard gluon. Their positions are shifted to the right in comparison with the proton–proton elastic scattering, as depicted in figure 7. Such a shift is a clear signal of the short-distance scale due to jets.

Measurements of $t$-distributions and their dynamics in the exclusive central diffraction could be used for the proposed investigations. To obtain the detailed diffractive pattern with dips for 1 GeV$^2 < -t < 5$ GeV$^2$ we need at least $10^4$ events for fixed (or falling within the small enough range of values) masses of the central system and $t$-resolution less than 10% in this region. At high luminosities the use of the missing mass method is limited below by central masses above 30 GeV because of the acceptance limitations and the absence of resonances with high rates in this region. That is why the only way is to use exclusive or semi-inclusive (exclusive+'soft' radiation in the central rapidity region) di-jet production. The best case is the measurements at the nominal luminosity at $\beta^* = 0.5$. Results are summarized in table 3.

## 5. Summary and conclusions

In this work we consider the exclusive double diffractive production $p + p \to p + M + p$, where $M$ is the particle or system of particles. The cross-section for this process was calculated in the Regge-eikonal approach plus SM process of the gluon–gluon fusion.

The first part of the paper is devoted to our new results on gamma–gamma production, taking into account different kinematical cuts. It was shown that we should be careful with the kinematics since this could lead to wrong predictions. Also two and three jet backgrounds were calculated for the Higgs production (in the $b\bar{b}$ mode) with the signal-to-background ratio $\sim$1. The main parameter $c_{gp}$ of the model is normalized to the new data from CDF. The data on exclusive gamma–gamma production from CDF show that the cross-section for Higgs boson production may be two times higher than predicted.

In the second part, we have proposed interesting measurements of $t$-distributions in the exclusive di-jet production at the LHC. The rate of di-jet production is large enough to obtain the diffractive pattern (with one dip around $t = -2.5$ GeV$^2$) in the region 0.01 GeV$^2 < |t| < 5$ GeV$^2$. From this pattern, we can obtain the transverse and longitudinal sizes of the interaction region and the ratio of real to imaginary parts of the amplitude.

## Acknowledgments

This work is supported by grants RFBR-06-02-16031 and INTAS-05-112-5481. We would like to thank Andrey Sobol for helpful discussions.

## References


[1] Petrov V A and Prokudin A V 2002 *Eur. Phys. J.* C **23** 135
[2] Petrov V A and Ryutin R A 2004 *J. High Energy Phys.*JHEP08(2004)013
[3] Eggert K, Oriunno M and Bozzo M 2004 *TOTEM Technical Design Report Preprint* CERN-LHCC-2004-002
Deile M 2005 *Czech. J. Phys.* **55** B757 (*Preprint* hep-ex/0503042)
[4] Bialas A and Landshoff P V 1991 *Phys. Lett.* B **256** 540
[5] Bzdak A 2005 *Phys. Lett.* B **615** 240
[6] Cudell J R and Hernandez O F 1996 *Nucl. Phys.* B **471** 471
[7] Pumplin J 1995 *Phys. Rev.* D **52** 1477
[8] Berera A and Collins J C 1996 *Nucl. Phys.* B **474** 183
[9] Shuryak E V and Zahed I 2003 *Phys. Rev.* D **68** 034001
[10] Kharzeev D and Levin E 2001 *Phys. Rev.* D **63** 073004
[11] Kozlov M, Levin E, Khachatryan V and Miller J 2007 *Nucl. Phys.* A **791** 382
[12] Gotsman E, Kowalski H, Levin E, Maor U and Prygarin A 2006 *Eur. Phys. J.* C **47** 655
[13] Khoze V A, Martin A D and Ryskin M G 2006 *Eur. Phys. J.* C **48** 467
[14] Close F E, Kirk A and Schuler G 2000 *Phys. Lett.* B **477** 13
[15] Troshin S M and Tyurin N E 2004 *Eur. Phys. J.* C **39** 435
[16] Boonekamp M, Roeck A, Peschanski R B and Royon C 2002 *Phys. Lett.* B **550** 93
[17] Cox B E, Loebinger F K and Pilkington A D 2007 *J. High Energy Phys.*JHEP10(2007)090
[18] Godizov A A and Petrov V A 2007 *J. High Energy Phys.*JHEP07(2007)083
[19] Petrov V A 1995 *Proc. Int. Conf. on Elastic and Diffractive Scattering (Blois)* (Frontiers in strong interactions) p 139
[20] Petrov V A, Prokudin A V and Ryutin R A 2005 *Czech. J. Phys.* **55** 17
[21] Donnachie A and Landshoff P V 2001 *Phys. Lett.* B **518** 63
[22] Khoze V A, Martin A D and Ryskin M G 2000 *Eur. Phys. J.* C **14** 525
Khoze V A, Martin A D and Ryskin M G 2001 *Eur. Phys. J.* C **21** 99
[23] Mesropian C *et al* 2006 *Preprint* FERMILAB-CONF-06-464-E
Goulianos K 2006 *Preprint* FERMILAB-CONF-06-464-E
Aaltonen T *et al* 2007 *Preprint* hep-ex/0712.0604
[24] Petrov V A, Ryutin R A, Sobol A E and Guillaud J-P 2005 *J. High Energy Phys.* JHEP06(2005)007
[25] Petrov V A, Ryutin R A, Sobol A E and Guillaud J-P 2007 *Preprint* 0711.1794
[26] Khoze V A, Martin A D, Ryskin M G and Stirling W J 2005 *Eur. Phys. J.* C **38** 475
[27] Gastmans R and Wu T T 1990 *The Ubiquitous Photon: Helicity Method for QED and QCD* (Oxford: Clarendon) p 1
[28] Albrow M 2006 Talk presented at *CMS Week (CERN)*
[29] Petrov V A, Prokudin A V, Troshin S M and Tyurin N E 2001 *J. Phys. G: Nucl. Part. Phys.* **27** 2225
[30] ZEUS Collaboration 2007 *PMC Phys.* A **1** 6
[31] Cheng H and Wu T T 1969 *Phys. Rev.* **183** 1324
[32] Bjorken J D 1971 *Preprint* SLAC-PUB-0905
[33] H1 Collaboration 2008 *Phys. Lett.* B **659** 796
[34] Goggi G *et al* 1978 *Phys. Lett.* B **79** 165